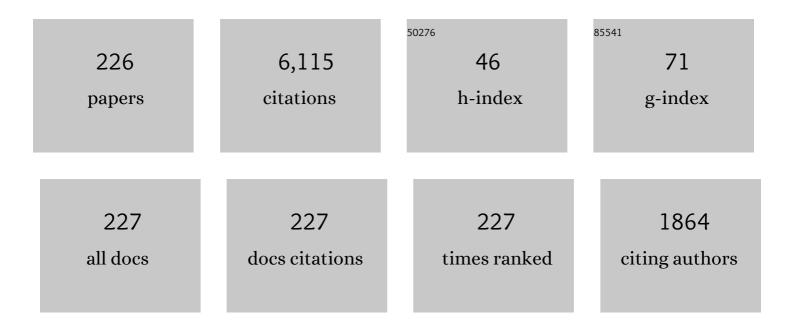
## Vincenzo Spagnolo

List of Publications by Year in descending order

Source: https://exaly.com/author-pdf/4726062/publications.pdf Version: 2024-02-01



#	Article	IF	CITATIONS
1	Application of standard and custom quartz tuning forks for quartz-enhanced photoacoustic spectroscopy gas sensing. Applied Spectroscopy Reviews, 2023, 58, 562-584.	6.7	6
2	Quartz-enhanced photoacoustic spectroscopy for multi-gas detection: A review. Analytica Chimica Acta, 2022, 1202, 338894.	5.4	79
3	Compact and portable quartz-enhanced photoacoustic spectroscopy sensor for carbon monoxide environmental monitoring in urban areas. Photoacoustics, 2022, 25, 100318.	7.8	45
4	Quartz tuning forks resonance frequency matching for laser spectroscopy sensing. Photoacoustics, 2022, 25, 100329.	7.8	87
5	Ppb-level gas detection using on-beam quartz-enhanced photoacoustic spectroscopy based on a 28ÂkHz tuning fork. Photoacoustics, 2022, 25, 100321.	7.8	57
6	Compact quartz-enhanced photoacoustic sensor for ppb-level ambient NO2 detection by use of a high-power laser diode and a grooved tuning fork. Photoacoustics, 2022, 25, 100325.	7.8	20
7	Mid-infrared intracavity quartz-enhanced photoacoustic spectroscopy with pptv – Level sensitivity using a T-shaped custom tuning fork. Photoacoustics, 2022, 25, 100330.	7.8	16
8	A novel double-tuning fork acoustic detection module for photoacoustic wide range sensing. , 2022, ,		0
9	Simultaneous measurement of N2O, CH4, and NH3 with a compact quartz-enhanced photoacoustic sensor for monitoring agricultural activities. , 2022, , .		1
10	Measurement of the methane isotopologues relaxation rate exploiting quartz-enhanced photoacoustic spectroscopy. , 2022, , .		1
11	Compact sensor for wide concentration range methane and ethane detection employing quartz tuning fork as photodetector in tunable diode laser spectroscopy. , 2022, , .		0
12	Quartz enhanced photoacoustic spectrometer for natural gas composition analysis. , 2022, , .		0
13	Quartz-enhanced photoacoustic spectroscopy employing a Vernier-effect distributed feedback-quantum cascade laser for multiple analytes detection. , 2022, , .		0
14	High-concentration methane and ethane QEPAS detection employing partial least squares regression to filter out energy relaxation dependence on gas matrix composition. Photoacoustics, 2022, 26, 100349.	7.8	41
15	Quartz-enhanced photoacoustic sensors for environmental monitoring applications. , 2022, , .		0
16	Quartz-enhanced photoacoustic NH3 sensor exploiting a large-prong-spacing quartz tuning fork and an optical fiber amplifier for biomedical applications. Photoacoustics, 2022, 26, 100363.	7.8	25
17	Ultra-highly sensitive HCI-LITES sensor based on a low-frequency quartz tuning fork and a fiber-coupled multi-pass cell. Photoacoustics, 2022, 27, 100381.	7.8	72
18	Modeling and Design of a Semi-Integrated QEPAS Sensor. Journal of Lightwave Technology, 2021, 39, 646-653.	4.6	3

#	Article	IF	CITATIONS
19	Broadband Gas QEPAS Detection Exploiting a Monolithic DFB-QCL Array. NATO Science for Peace and Security Series B: Physics and Biophysics, 2021, , 61-70.	0.3	0
20	Multi-pass quartz-enhanced photoacoustic spectroscopy-based trace gas sensing. Optics Letters, 2021, 46, 977.	3.3	52
21	H2S quartz-enhanced photoacoustic spectroscopy sensor employing a liquid-nitrogen-cooled THz quantum cascade laser operating in pulsed mode. Photoacoustics, 2021, 21, 100219.	7.8	37
22	Quartz-enhanced photoacoustic spectroscopy exploiting low-frequency tuning forks as a tool to measure the vibrational relaxation rate in gas species. Photoacoustics, 2021, 21, 100227.	7.8	43
23	Quartz-enhanced photoacoustic spectroscopy of methane isotopologues. , 2021, , .		О
24	Quartz-enhanced photoacoustic spectroscopy for CO detection in SF6 decomposition. , 2021, , .		0
25	Quartz tuning forks employed as photodetectors in TDLAS sensors. , 2021, , .		Ο
26	Parts-per-billion detection of carbon monoxide: A comparison between quartz-enhanced photoacoustic and photothermal spectroscopy. Photoacoustics, 2021, 22, 100244.	7.8	34
27	Ppt level carbon monoxide detection based on light-induced thermoelastic spectroscopy exploring custom quartz tuning forks and a mid-infrared QCL. Optics Express, 2021, 29, 25100.	3.4	76
28	Influence of Air Pressure on the Resonance Properties of a T-Shaped Quartz Tuning Fork Coupled with Resonator Tubes. Applied Sciences (Switzerland), 2021, 11, 7974.	2.5	6
29	High and flat spectral responsivity of quartz tuning fork used as infrared photodetector in tunable diode laser spectroscopy. Applied Physics Reviews, 2021, 8, .	11.3	76
30	Phytoextraction of Cr(VI)-Contaminated Soil by Phyllostachys pubescens: A Case Study. Toxics, 2021, 9, 312.	3.7	10
31	Ultra-high sensitive trace gas detection based on light-induced thermoelastic spectroscopy and a custom quartz tuning fork. Applied Physics Letters, 2020, 116, .	3.3	90
32	Broadband detection of methane and nitrous oxide using a distributed-feedback quantum cascade laser array and quartz-enhanced photoacoustic sensing. Photoacoustics, 2020, 17, 100159.	7.8	47
33	Quartz-enhanced photoacoustic spectroscopy for gas sensing applications. , 2020, , 597-659.		4
34	New Developments in Quartz-Enhanced Photoacoustic Sensing Real-World Applications. , 2020, , .		2
35	Partial Least-Squares Regression as a Tool to Retrieve Gas Concentrations in Mixtures Detected Using Quartz-Enhanced Photoacoustic Spectroscopy. Analytical Chemistry, 2020, 92, 11035-11043.	6.5	42
36	Mid-Infrared Quartz-Enhanced Photoacoustic Sensor for ppb-Level CO Detection in a SF <sub>6</sub> Gas Matrix Exploiting a T-Grooved Quartz Tuning Fork. Analytical Chemistry, 2020, 92, 13922-13929.	6.5	42

#	Article	IF	CITATIONS
37	Fiber-Coupled Quartz-Enhanced Photoacoustic Spectroscopy System for Methane and Ethane Monitoring in the Near-Infrared Spectral Range. Molecules, 2020, 25, 5607.	3.8	28
38	Phytoextraction from Chromium-Contaminated Soil Using Moso Bamboo in Mediterranean Conditions. Water, Air, and Soil Pollution, 2020, 231, 1.	2.4	11
39	Quartz-Enhanced Photoacoustic Detection of Ethane in the Near-IR Exploiting a Highly Performant Spectrophone. Applied Sciences (Switzerland), 2020, 10, 2447.	2.5	11
40	Front-End Amplifiers for Tuning Forks in Quartz Enhanced PhotoAcoustic Spectroscopy. Applied Sciences (Switzerland), 2020, 10, 2947.	2.5	16
41	Environmental Monitoring of Methane with Quartz-Enhanced Photoacoustic Spectroscopy Exploiting an Electronic Hygrometer to Compensate the H2O Influence on the Sensor Signal. Sensors, 2020, 20, 2935.	3.8	29
42	Quartz-enhanced photoacoustic spectroscopy for hydrocarbon trace gas detection and petroleum exploration. Fuel, 2020, 277, 118118.	6.4	43
43	In-plane quartz-enhanced photoacoustic spectroscopy. Applied Physics Letters, 2020, 116, .	3.3	59
44	Photoacoustic spectroscopy for gas sensing: A comparison between piezoelectric and interferometric readout in custom quartz tuning forks. Photoacoustics, 2020, 17, 100155.	7.8	19
45	Sub-ppb-level CH <sub>4</sub> detection by exploiting a low-noise differential photoacoustic resonator with a room-temperature interband cascade laser. Optics Express, 2020, 28, 19446.	3.4	27
46	Light-induced thermo-elastic effect in quartz tuning forks exploited as a photodetector in gas absorption spectroscopy. Optics Express, 2020, 28, 19074.	3.4	51
47	Measurement of non-radiative gas molecules relaxation rates by using quartz-enhanced photoacoustic spectroscopy. , 2020, , .		0
48	Intracavity quartz-enhanced photoacoustic spectroscopy for CO/N2O detection in the part-per-trillion concentration range. , 2020, , .		0
49	Fiber-coupled quartz-enhanced photoacoustic sensor for methane and ethane trace detection. , 2020, ,		Ο
50	Partial least squares regression as novel tool for gas mixtures analysis in quartz-enhanced photoacoustic spectroscopy. , 2020, , .		3
51	N2-cooled THz quartz-enhanced photoacoustic sensor operating in pulsed mode for hydrogen sulfide detection in the part-per-billion concentration range. , 2020, , .		Ο
52	Comparison between interferometric and piezoelectric readout of tuning fork vibrations in quartz-enhanced photoacoustic spectroscopy. , 2020, , .		0
53	Atmospheric CH4 measurement near a landfill using an ICL-based QEPAS sensor with V-T relaxation self-calibration. Sensors and Actuators B: Chemical, 2019, 297, 126753.	7.8	127
54	Dual-Gas Quartz-Enhanced Photoacoustic Sensor for Simultaneous Detection of Methane/Nitrous Oxide and Water Vapor. Analytical Chemistry, 2019, 91, 12866-12873.	6.5	53

#	Article	IF	CITATIONS
55	Acoustic Coupling between Resonator Tubes in Quartz-Enhanced Photoacoustic Spectrophones Employing a Large Prong Spacing Tuning Fork. Sensors, 2019, 19, 4109.	3.8	26
56	Damping Mechanisms of Piezoelectric Quartz Tuning Forks Employed in Photoacoustic Spectroscopy for Trace Gas Sensing. Physica Status Solidi (A) Applications and Materials Science, 2019, 216, 1800552.	1.8	13
57	Ppb-Level Quartz-Enhanced Photoacoustic Detection of Carbon Monoxide Exploiting a Surface Grooved Tuning Fork. Analytical Chemistry, 2019, 91, 5834-5840.	6.5	67
58	Simultaneous multi-gas detection between 3 and 4 μm based on a 2.5-m multipass cell and a tunable Fabry-Pérot filter detector. Spectrochimica Acta - Part A: Molecular and Biomolecular Spectroscopy, 2019, 216, 154-160.	3.9	9
59	Influence of Tuning Fork Resonance Properties on Quartz-Enhanced Photoacoustic Spectroscopy Performance. Sensors, 2019, 19, 3825.	3.8	3
60	Methane, ethane and propane detection using a compact quartz enhanced photoacoustic sensor and a single interband cascade laser. Sensors and Actuators B: Chemical, 2019, 282, 952-960.	7.8	66
61	Tuning forks with optimized geometries for quartz-enhanced photoacoustic spectroscopy. Optics Express, 2019, 27, 1401.	3.4	77
62	Quartz-enhanced photoacoustic sensor for ethylene detection implementing optimized custom tuning fork-based spectrophone. Optics Express, 2019, 27, 4271.	3.4	46
63	Piezo-enhanced acoustic detection module for mid-infrared trace gas sensing using a grooved quartz tuning fork. Optics Express, 2019, 27, 35267.	3.4	12
64	New generation of tuning forks for quartz-enhanced photoacoustic spectroscopy. , 2019, , .		0
65	Quartz-enhanced photoacoustic sensors for detection of multiple hydrocarbon and methane isotopes. , 2019, , .		0
66	Octupole electrode pattern for tuning forks vibrating at the first overtone mode in quartz-enhanced photoacoustic spectroscopy. , 2019, , .		0
67	Simultaneous dual gas QEPAS sensing of water and methane/nitrous oxide. , 2019, , .		1
68	Quartz-enhanced photoacoustic spectroscopy employing a distributed feedback-quantum cascade laser array for nitrous oxide and methane broadband detection. , 2019, , .		0
69	Recent advances in quartz enhanced photoacoustic sensing. Applied Physics Reviews, 2018, 5, .	11.3	174
70	Nitrous oxide quartz-enhanced photoacoustic detection employing a broadband distributed-feedback quantum cascade laser array. Applied Physics Letters, 2018, 113, .	3.3	34
71	Octupole electrode pattern for tuning forks vibrating at the first overtone mode in quartz-enhanced photoacoustic spectroscopy. Optics Letters, 2018, 43, 1854.	3.3	20
72	Loss Mechanisms Determining the Quality Factors in Quartz Tuning Forks Vibrating at the Fundamental and First Overtone Modes. IEEE Transactions on Ultrasonics, Ferroelectrics, and Frequency Control, 2018, 65, 1951-1957.	3.0	29

#	Article	IF	CITATIONS
73	Fiber-ring laser intracavity QEPAS gas sensor using a 7.2†kHz quartz tuning fork. Sensors and Actuators B: Chemical, 2018, 268, 512-518.	7.8	46
74	Compact and low-noise quartz-enhanced photoacoustic sensor for sub-ppm ethylene detection in atmosphere. , 2018, , .		2
75	Tapered hollow-core fibers providing single-mode output in the 3.5um-7.8um spectral range. , 2018, , .		Ο
76	Interband cascade laser based quartz-enhanced photoacoustic sensor for multiple hydrocarbons detection. , 2018, , .		1
77	Recent advances in quartz-enhanced photoacoustic sensing. , 2018, , .		2
78	High Performance Mid-IR Devices and Applications to Gas Sensing. , 2018, , .		0
79	Fiber Laser Intracavity Quartz-Enhanced Photoacoustic Gas Sensor. , 2018, , .		0
80	New Developments in Quartz-Enhanced Photoacoustic Spectroscopy for Gas Sensing Applications. , 2018, , .		0
81	Quartz–enhanced photoacoustic spectrophones exploiting custom tuning forks: a review. Advances in Physics: X, 2017, 2, 169-187.	4.1	44
82	Pure amplitude and wavelength modulation spectroscopy for detection of N2O using a three-section quantum cascade laser. , 2017, , .		0
83	Low power consumption quartz-enhanced photoacoustic gas sensor employing a quantum cascade laser in pulsed operation. Proceedings of SPIE, 2017, , .	0.8	Ο
84	Double antinode excited quartz-enhanced photoacoustic spectrophone. Applied Physics Letters, 2017, 110, .	3.3	33
85	Single-tube on beam quartz-enhanced photoacoustic spectrophones exploiting a custom quartz tuning fork operating in the overtone mode. Proceedings of SPIE, 2017, , .	0.8	Ο
86	Simultaneous dual-gas QEPAS detection based on a fundamental and overtone combined vibration of quartz tuning fork. Applied Physics Letters, 2017, 110, .	3.3	64
87	Mode matching of a laser-beam to a compact high finesse bow-tie optical cavity for quartz enhanced photoacoustic gas sensing. Sensors and Actuators A: Physical, 2017, 267, 70-75.	4.1	7
88	Recent advances in quartz-enhanced photoacoustic sensors employing custom tuning fork operating at the first overtone flexural mode. , 2017, , .		0
89	Recent advances in quartz enhanced photoacoustic sensing. , 2017, , .		0
90	Trace gas spectroscopy using state-of-the- art mid-infrared semiconductor laser sources: progress, status, and applications. , 2017, , .		0

#	Article	IF	CITATIONS
91	Improved Tuning Fork for Terahertz Quartz-Enhanced Photoacoustic Spectroscopy. Sensors, 2016, 16, 439.	3.8	59
92	Low-Loss Coupling of Quantum Cascade Lasers into Hollow-Core Waveguides with Single-Mode Output in the 3.7–7.6 μm Spectral Range. Sensors, 2016, 16, 533.	3.8	21
93	Highly sensitive gas leak detector based on a quartz-enhanced photoacoustic SF6 sensor. Optics Express, 2016, 24, 15872.	3.4	57
94	Purely wavelength- and amplitude-modulated quartz-enhanced photoacoustic spectroscopy. Optics Express, 2016, 24, 25943.	3.4	44
95	Mid infrared quantum cascade laser operating in pure amplitude modulation for background-free trace gas spectroscopy. Optics Express, 2016, 24, 26464.	3.4	11
96	New spectrophone designs based on a quartz tuning fork. , 2016, , .		0
97	Recent advances of the quartz-enhanced photoacoustic trace gas detection technique. , 2016, , .		0
98	Overtone resonance enhanced single-tube on-beam quartz enhanced photoacoustic spectrophone. Applied Physics Letters, 2016, 109, .	3.3	46
99	Innovative quartz enhanced photoacoustic sensors for trace gas detection. , 2016, , .		2
100	Analysis of overtone flexural modes operation in quartz-enhanced photoacoustic spectroscopy. Optics Express, 2016, 24, A682.	3.4	57
101	New developments in THz quartz enhanced photoacoustic spectroscopy. , 2016, , .		1
102	Allan Deviation Plot as a Tool for Quartz-Enhanced Photoacoustic Sensors Noise Analysis. IEEE Transactions on Ultrasonics, Ferroelectrics, and Frequency Control, 2016, 63, 555-560.	3.0	72
103	Hollow-core waveguide for single-mode laser beam propagation in the spectral range of 3.7-7.3 $\hat{l}$ /4m. , 2016, , .		Ο
104	Quartz enhanced photoacoustic leak sensor for mechatronic components. Proceedings of SPIE, 2016, ,	0.8	0
105	Quartz tuning forks with novel geometries for optoacoustic gas sensing. , 2016, , .		Ο
106	Single-tube on-beam quartz-enhanced photoacoustic spectroscopy. Optics Letters, 2016, 41, 978.	3.3	88
107	Analysis of the electro-elastic properties of custom quartz tuning forks for optoacoustic gas sensing. Sensors and Actuators B: Chemical, 2016, 227, 539-546.	7.8	110
108	Recent advances of mid–infrared compact, field deployable sensors and their real world applications in the petrochemical industry, atmospheric chemistry and security. , 2016, , .		0

#	Article	IF	CITATIONS
109	Micro-resonator Parameter Optimization of a QEPAS Spectrophone using a Custom Quartz Tuning Fork with large Prong Spacing. , 2016, , .		0
110	Recent advances and applications of mid-infrared semiconductor based trace gas sensor technologies. , 2016, , .		0
111	Hollow core waveguide as mid-infrared laser modal beam filter. Journal of Applied Physics, 2015, 118, 113102.	2.5	20
112	Quartz-enhanced photoacoustic spectroscopy exploiting tuning fork overtone modes. Applied Physics Letters, 2015, 107, .	3.3	61
113	A quartz-enhanced photoacoustic sensor for H2S trace-gas detection at 2.6Âμm. Applied Physics B: Lasers and Optics, 2015, 119, 21-27.	2.2	37
114	Quartz-enhanced photoacoustic sensors for H2S trace gas detection. , 2015, , .		1
115	New approaches in quartz-enhanced photoacoustic sensing. Proceedings of SPIE, 2015, , .	0.8	2
116	THz Quartz-enhanced photoacoustic sensor for H_2S trace gas detection. Optics Express, 2015, 23, 7574.	3.4	76
117	Single mode operation with mid-IR hollow fibers in the range 51-105 µm. Optics Express, 2015, 23, 195.	3.4	32
118	Quartz enhanced photoacoustic H2S gas sensor based on a fiber-amplifier source and a custom tuning fork with large prong spacing. Applied Physics Letters, 2015, 107, .	3.3	128
119	Mid-IR quantum cascade laser mode coupling in hollow-core, fiber-optic waveguides with single-mode beam delivery. Proceedings of SPIE, 2015, , .	0.8	3
120	High finesse optical cavity coupled with a quartz-enhanced photoacoustic spectroscopic sensor. Analyst, The, 2015, 140, 736-743.	3.5	41
121	Modeling the dependence of fork geometry on the performance of quartz enhanced photoacoustic spectroscopic sensors. , 2015, , .		1
122	Measurement of relative velocity of independent targets by a quantum cascade laser subject to optical feedback. , 2014, , .		0
123	Atmospheric CH_4 and N_2O measurements near Greater Houston area landfills using a QCL-based QEPAS sensor system during DISCOVER-AQ 2013. Optics Letters, 2014, 39, 957.	3.3	62
124	Widely-tunable mid-infrared fiber-coupled quartz-enhanced photoacoustic sensor for environmental monitoring. Optics Express, 2014, 22, 28222.	3.4	93
125	Hydrogen peroxide detection with quartz-enhanced photoacoustic spectroscopy using a distributed-feedback quantum cascade laser. Applied Physics Letters, 2014, 104, .	3.3	44
126	Quartz-Enhanced Photoacoustic Spectroscopy: A Review. Sensors, 2014, 14, 6165-6206.	3.8	336

#	Article	IF	CITATIONS
127	A quartz enhanced photo-acoustic gas sensor based on a custom tuning fork and a terahertz quantum cascade laser. Analyst, The, 2014, 139, 2079-2087.	3.5	77
128	Intracavity quartz-enhanced photoacoustic sensor. Applied Physics Letters, 2014, 104, .	3.3	115
129	Quartz Enhanced Photoacoustic Sensors for Trace Gas Detection in the IR and THz Spectral Range. NATO Science for Peace and Security Series B: Physics and Biophysics, 2014, , 139-151.	0.3	0
130	Terahertz quartz enhanced photo-acoustic sensor. Applied Physics Letters, 2013, 103, .	3.3	107
131	Hot Electrons in THz Quantum Cascade Lasers. Journal of Infrared, Millimeter, and Terahertz Waves, 2013, 34, 357-373.	2.2	7
132	On Line Sensing of Ultrafast Laser Microdrilling Processes by Optical Feedback Interferometry. Physics Procedia, 2013, 41, 670-676.	1.2	6
133	THz quartz-enhanced photoacoustic sensor employing a quantum cascade laser source. Proceedings of SPIE, 2013, , .	0.8	2
134	Electronic temperature in phonon-photon-phonon terahertz quantum cascade devices with high-operating temperature performance. , 2013, , .		0
135	Mid-infrared fiber-coupled QCL-QEPAS sensor. Applied Physics B: Lasers and Optics, 2013, 112, 25-33.	2.2	66
136	Low-Loss Hollow Waveguide Fibers for Mid-Infrared Quantum Cascade Laser Sensing Applications. Sensors, 2013, 13, 1329-1340.	3.8	42
137	Part-per-trillion level detection of SF <sub>6</sub> using a single-mode fiber-coupled quantum cascade laser and a quartz enhanced photoacoustic sensor. Proceedings of SPIE, 2013, , .	0.8	Ο
138	Spatial mode filtering of mid-infrared (mid-IR) laser beams with hollow core fiber optics. Proceedings of SPIE, 2013, , .	0.8	8
139	Electronic temperatures of terahertz quantum cascade active regions with phonon scattering assisted injection and extraction scheme. Optics Express, 2013, 21, 10172.	3.4	8
140	Cavity and quartz enhanced photo-acoustic mid-IR sensor. , 2013, , .		1
141	Quantum cascade laser-based sensing to investigate fast laser ablation process. , 2013, , .		Ο
142	THz quantum cascade laser-based quartz enhanced photo-acoustic sensor. , 2013, , .		1
143	Quantum cascade laser-based sensor system for hydrogen peroxide detection. , 2013, , .		0
144	Sensitive detection of nitric oxide using a 5.26 μm external cavity quantum cascade laser based QEPAS sensor. Proceedings of SPIE, 2012, , .	0.8	9

#	Article	IF	CITATIONS
145	Modulation cancellation method for isotope ^180/^160 ratio measurements in water. Optics Express, 2012, 20, 3401.	3.4	23
146	Part-per-trillion level SF_6 detection using a quartz enhanced photoacoustic spectroscopy-based sensor with single-mode fiber-coupled quantum cascade laser excitation. Optics Letters, 2012, 37, 4461.	3.3	142
147	Coupling external cavity mid-IR quantum cascade lasers with low loss hollow metallic/dielectric waveguides. Applied Physics B: Lasers and Optics, 2012, 108, 255-260.	2.2	27
148	Spectroscopic measurements of isotopic water composition using a new modulation cancellation method. , 2012, , .		0
149	Detection of ultrafast laser ablation using quantum cascade laser-based sensing. Applied Physics Letters, 2012, 101, .	3.3	18
150	Sensitive Detection of Nitric Oxide Using a Quantum Cascade Laser Based QEPAS Sensor. , 2012, , .		1
151	Modulation cancellation method for spectroscopic measurements. , 2012, , .		0
152	Mid-infrared quantum cascade laser based trace gas sensor technologies: Recent advances and applications. , 2011, , .		0
153	Quantum-cascade-laser-based optoacoustic detection for breath sensor applications. , 2011, , .		5
154	Mid-infrared quantum cascade laser based trace gas technologies: Recent progress and applications in health and environmental monitoring. , 2011, , .		2
155	Ppb-level detection of nitric oxide using an external cavity quantum cascade laser based QEPAS sensor. Optics Express, 2011, 19, 24037.	3.4	122
156	Modulation cancellation method for measurements of small temperature differences in a gas. Optics Letters, 2011, 36, 460.	3.3	23
157	Modulation cancellation method for laser spectroscopy. , 2011, , .		0
158	Modulation cancellation method (MOCAM) in modulation spectroscopy. , 2011, , .		1
159	Modulation cancellation method in laser spectroscopy. Applied Physics B: Lasers and Optics, 2011, 103, 735-742.	2.2	20
160	Quantum Cascade Laser Technology for the Ultrasensitive Detection of Low-Level Nitric Oxide. Methods in Molecular Biology, 2011, 704, 115-133.	0.9	2
161	Quantum-cascade-laser-based optoacoustic detection: application to nitric oxide and formaldehyde. Proceedings of SPIE, 2010, , .	0.8	0
162	Trace gas sensing using quantum cascade lasers and a fiber-coupled optoacoustic sensor: Application to formaldehyde. Journal of Physics: Conference Series, 2010, 214, 012037.	0.4	5

#	Article	IF	CITATIONS
163	NO trace gas sensor based on quartz-enhanced photoacoustic spectroscopy and external cavity quantum cascade laser. Applied Physics B: Lasers and Optics, 2010, 100, 125-130.	2.2	131
164	Advanced optoacoustic sensor designs for environmental applications. Proceedings of SPIE, 2010, , .	0.8	0
165	Time of flight measurements of the nanoscale heat transfer dynamic in terahertz quantum cascade lasers. , 2009, , .		0
166	Hot electron effects and nanoscale heat transfer in Terahertz quantum cascade lasers. Proceedings of SPIE, 2009, , .	0.8	2
167	Photoacoustic trace gas sensing with mid-IR quantum cascade lasers. , 2009, , .		1
168	Quantum Cascade Laser-Based Photoacoustic Sensor for Trace Detection of Formaldehyde Gas. Sensors, 2009, 9, 2697-2705.	3.8	36
169	Optical and Electronic NOx Sensors for Applications in Mechatronics. Sensors, 2009, 9, 3337-3356.	3.8	25
170	Trace gas sensing using quantum cascade lasers and optoacoustic detection. Proceedings of SPIE, 2009, , .	0.8	0
171	Photoacoustic Techniques for Trace Gas Sensing Based on Semiconductor Laser Sources. Sensors, 2009, 9, 9616-9628.	3.8	182
172	Nanoscale heat transfer in quantum cascade lasers. Physica E: Low-Dimensional Systems and Nanostructures, 2008, 40, 1780-1784.	2.7	25
173	Temperature Dependence of Thermal Conductivity and Boundary Resistance in THz Quantum Cascade Lasers. IEEE Journal of Selected Topics in Quantum Electronics, 2008, 14, 431-435.	2.9	52
174	Thermal Modeling of Terahertz Quantum-Cascade Lasers: Comparison of Optical Waveguides. IEEE Journal of Quantum Electronics, 2008, 44, 680-685.	1.9	38
175	Improved thermal management of mid-IR quantum cascade lasers. Journal of Applied Physics, 2008, 103, .	2.5	35
176	Microprobe photoluminescence assessment of the wall-plug efficiency in interband cascade lasers. Journal of Applied Physics, 2008, 104, 046101.	2.5	1
177	Time-resolved measurement of the local lattice temperature in terahertz quantum cascade lasers. Applied Physics Letters, 2008, 92, 101116.	3.3	28
178	Correlation between the subband electronic temperatures and the internal quantum efficiency of THz quantum cascade lasers. , 2008, , .		0
179	Experimental Investigation of Hot Carriers in Terahertz Quantum Cascade Lasers. Acta Physica Polonica A, 2008, 113, 787-794.	0.5	0
180	Influence of InAs, AlAs δlayers on the optical, electronic, and thermal characteristics of strain-compensated GalnAsâ`•AlInAs quantum-cascade lasers. Applied Physics Letters, 2007, 91, .	3.3	43

#	Article	IF	CITATIONS
181	Experimental investigation of the lattice and electronic temperatures in Ga0.47In0.53Asâ^•Al0.62Ga0.38As1â^'xSbx quantum-cascade lasers. Applied Physics Letters, 2007, 90, 121109.	3.3	24
182	Terahertz quantum cascade lasers with large wall-plug efficiency. Applied Physics Letters, 2007, 90, 191115.	3.3	60
183	Experimental measurement of the wall-plug efficiency in THz quantum cascade lasers. , 2007, , .		0
184	Electronic and thermal properties of Sb-based QCLs operating in the first atmospheric window. , 2007,		1
185	High performance THz quantum cascade laser with different optical waveguide configurations. , 2007,		0
186	Hot-phonon generation in THz quantum cascade lasers. Journal of Physics: Conference Series, 2007, 92, 012018.	0.4	8
187	Electronic and Thermal properties of THz Quantum Cascade. , 2006, , .		0
188	Thermal properties of THz quantum cascade lasers based on different optical waveguide configurations. Applied Physics Letters, 2006, 89, 021111.	3.3	46
189	Non equilibrium electrons in THz quantum cascade lasers. , 2006, 6133, 126.		3
190	Electronic and lattice temperatures in bound-to-continuum terahertz quantum cascade lasers. , 2006, , .		1
191	Subband electronic temperatures and electron-lattice energy relaxation in terahertz quantum cascade lasers with different conduction band offsets. Applied Physics Letters, 2006, 89, 131114.	3.3	32
192	Electron-lattice coupling in bound-to-continuum THz quantum-cascade lasers. Applied Physics Letters, 2006, 88, 241109.	3.3	38
193	Thermal modeling of GalnAsâ^•AlInAs quantum cascade lasers. Journal of Applied Physics, 2006, 100, 043109.	2.5	73
194	Measurement of subband electronic temperatures and population inversion in THz quantum-cascade lasers. Applied Physics Letters, 2005, 86, 111115.	3.3	123
195	Electronic spatial distribution of In0.53Ga0.47Asâ^•AlAs0.56Sb0.44 quantum-cascade lasers. Journal of Applied Physics, 2005, 98, 086106.	2.5	1
196	Influence of the band-offset on the electronic temperature of GaAs/Al(Ga)As superlattice quantum cascade lasers. Semiconductor Science and Technology, 2004, 19, S110-S112.	2.0	17
197	Simultaneous measurement of the electronic and lattice temperatures in GaAs/Al0.45Ga0.55As quantum-cascade lasers: Influence on the optical performance. Applied Physics Letters, 2004, 84, 3690-3692.	3.3	70
198	Experimental determination of the temperature distribution in trench-confined oxide vertical-cavity surface-emitting lasers. IEEE Journal of Quantum Electronics, 2003, 39, 701-707.	1.9	15

#	Article	IF	CITATIONS
199	Thermal characteristics of quantum-cascade lasers by micro-probe optical spectroscopy. IEE Proceedings: Optoelectronics, 2003, 150, 298.	0.8	22
200	Thermoelastic stress in GaAs/AlGaAs quantum cascade lasers. Applied Physics Letters, 2003, 82, 4639-4641.	3.3	15
201	Direct measurement of the local temperature distribution in oxide VCSELs. , 2002, , .		4
202	<title>Optical sensor for real-time weld defect detection</title> ., 2002,,.		5
203	Nonequilibrium optical phonon generation by steady-state electron transport in quantum-cascade lasers. Applied Physics Letters, 2002, 80, 4303-4305.	3.3	25
204	2-D temperature mapping of vertical-cavity surface-emitting lasers determined by microprobe electroluminescence. IEEE Photonics Technology Letters, 2002, 14, 266-268.	2.5	1
205	<title>Nondestructive technique for the direct measurement of the local temperature distribution in VCSELs</title> . , 2002, 4648, 22.		3
206	Thermal resistance and temperature characteristics of GaAs/Al0.33Ga0.67As quantum-cascade lasers. Applied Physics Letters, 2001, 78, 1177-1179.	3.3	33
207	Optical sensor for real-time monitoring of CO_2 laser welding process. Applied Optics, 2001, 40, 6019.	2.1	107
208	<title>Peak optical power and thermal performance of quantum cascade lasers</title> ., 2001, , .		0
209	Facet temperature mapping of GaAs/AlGaAs quantum cascade lasers by photoluminescence microprobe. Optical Materials, 2001, 17, 219-222.	3.6	4
210	Temperature profile of GaInAs/AlInAs/InP quantum cascade-laser facets measured by microprobe photoluminescence. Applied Physics Letters, 2001, 78, 2095-2097.	3.3	58
211	Electronic distribution in superlattice quantum cascade lasers. Applied Physics Letters, 2000, 77, 1088-1090.	3.3	27
212	Evidence of electronic confinement in pseudomorphic Si/GaAs superlattices. Physical Review B, 1998, 57, R15100-R15103.	3.2	3
213	Quantum-well-laser mirror degradation investigated by microprobe optical spectroscopy. , 1995, , .		1
214	Fröhlich electron-phonon interaction in CdSxSe1-xnanocrystals. Superlattices and Microstructures, 1995, 18, 113-120.	3.1	6
215	One- and two-phonon scattering processes in ZnSe/ZnSxSe1â^'xsuperlattices studied by micro-Raman spectroscopy. Physical Review B, 1994, 50, 4988-4991.	3.2	1
216	Well width dependence of electron-phonon interaction in ZnSe/ZnSxSe1-x superlattices determined by micro-raman spectroscopy. Superlattices and Microstructures, 1994, 16, 47-49.	3.1	0

#	Article	IF	CITATIONS
217	Raman scattering in CdTe1-xSex and CdS1-xSex nanocrystals embedded in glass. Superlattices and Microstructures, 1994, 16, 51-54.	3.1	27
218	Si-GaAs(001) superlattice structure. Journal of Crystal Growth, 1993, 127, 121-125.	1.5	12
219	Phonons in Si/GaAs superlattices. Physical Review B, 1992, 46, 7296-7299.	3.2	13
220	Siâ€GaAs(001) superlattices. Applied Physics Letters, 1992, 61, 1570-1572.	3.3	10
221	Excitons and electron-phonon interaction in In0.52Ga0.18Al0.30As layers. Solid State Communications, 1992, 84, 679-683.	1.9	6
222	Vibrational properties of Si/GaAs superlattices. Superlattices and Microstructures, 1992, 12, 429-432.	3.1	2
223	State of the art of InP and GaAs quantum cascade lasers. , 0, , .		О
224	Simultaneous measurement of the electronic and lattice temperatures in GaAs quantum cascade lasers and their correlation with the optical performance. , 0, , .		0
225	Modulation-cancellation method for laser spectroscopy. SPIE Newsroom, 0, , .	0.1	0
226	Compact and Versatile QEPAS-Based Sensor Box for Simultaneous Detection of Methane and Infrared Absorber Gas Molecules in Ambient Air. Frontiers in Environmental Chemistry, 0, 3, .	1.6	7